Pore network as a model of porous media: Comparison between nonhierarchical and hierarchical organizations of pores

Radim Vočka* and Marc A. Dubois†
Service de Physique de l'Etat Condensé, SPEC/DRECAM, CEN Saclay, F-91191 Gif-sur-Yvette, France
(Received 16 December 1998; revised manuscript received 2 June 2000)

A pore network is used as a model of a porous medium with hierarchical and single level organization of the pores. A microscopic diffusion or adsorption process is introduced that permits the study of both temporal evolution and effective properties of transport. The relationships between the model parameters and the measurable quantities are derived. The transport in media with a hierarchical organization of pores is shown to be qualitatively different from that in media lacking this organization. The question of experimental distinction between the two types of pore organization is also studied. We show that mercury intrusion porosimetry (MIP) measurements furnish valuable information about the pore organization in a sample, but that the exact deconvolution of the real pore size distribution from the experimental data is not straightforward. Our work provides indications for a correct interpretation of MIP results. Qualitative comparison with experiments show the pertinence of hierarchical models.

PACS number(s): 81.05.Rm

I. INTRODUCTION

A lot of effort has been devoted to the study of transport properties of porous materials, motivated by a large number of applications reaching from oil recovery and ground water contamination to diffusion in biological membranes. Along with the experimental work, modeling is an important tool, which allows generalization of the experimental results and also gives a better insight into the transport process itself, because its important features can be independently studied. This enhances the interpretation of experimental data.

Models based on a simplified structure of porous media are useful from this point of view. The oldest, representing the porous media as a packing of spheres, dates from the 19th century. Nevertheless, these models are difficult to handle both analytically and numerically, and they have gained renewed attention recently as ''continuum percolation models'' [1,2].

An important simplification has come with the network models introduced by Fatt [3], which have become very popular [4,5]. In these, the pores are represented as tubes of a given diameter which are placed on a regular network, generally in a rectangular or cubic grid. This approach can be viewed as a generalization of percolation models [6]. The drawback of the simple network models is that they represent only single pore-level structures, since all the pores have the same length. In this case one family of pores determines the transport properties, which makes this model suitable for only the limited number of materials that fulfill this one-level requirement. It has been applied with success to permeability of sandstone, for example, where the pertinent pore diameter is determined from the section of throats between the grains [7].

This approach is inadequate for materials with a hierarchical structure that contain several families of pores of different length scales (macroporosity, microporosity), such as mortar, fractured media, or several types of rock [8]. In hierarchical structures two points in a sample can be connected by two different paths formed exclusively by micropores or by macropores, each of which has an influence on the transport properties. A first approach to this problem was considered in [9,10]: a network model was proposed, where neighbor sites are connected by several transport paths of different conductivities, each path corresponding to a given family of pores. Pores forming different paths are not actually represented. Exchange between various transport paths is possible only at the sites of the network; therefore all the transport paths have *a priori* the same length. Hence this approach is not sufficient for the case where more than two families of pores participate in the transport. In more realistic models pores forming different transport paths are explicitly represented. A hierarchical structure is typically obtained by introducing the correlations between the pore length and the pore diameter. They are generated by fractional Brownian motion [11,12], or by a fractal-type construction of a model [13–16]. This second possibility, directly motivated by the observation that the porous medium is scale invariant in certain length ranges [17], has the advantage that as well as a numerical description an analytical approach is possible. These models are often used for modeling transport on a geological scale, so a large number of pore families is represented. Nevertheless, for most examples of porous materials on a laboratory scale, just two or three pore families are sufficient [18,19].

Even though much work has been done on pore network models, a comprehensive comparison of transport in porous media with the ''single level'' and ''multiscale'' pore structure is still lacking. A shortcoming of current transport studies, moreover, is that adsorption is not explicitly considered. We argue that this approach does not lead to the correct description of the temporal evolution of transport processes, because diffusion and adsorption coefficients have different dependencies on the pore diameter. From this logic we de-

*Email address: vor@nri.cz
†Email address: mad@spec.saclay.cea.fr

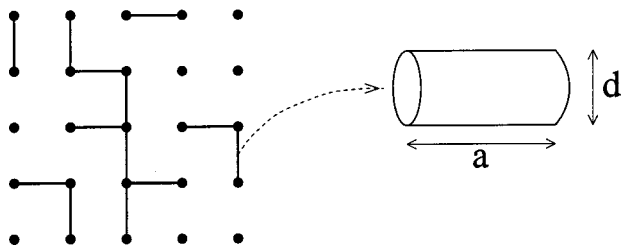

FIG. 1. Single level network. Sites (●) and pores (horizontal line) of non-null diameter. A pore has the form of a cylinder of length a and diameter d.

velop a description of microscopic diffusion process with adsorption in a pore network model. We find the relation with the macroscopic diffusion equation in porous media, which allows us to connect the transition rates of the microscopic processes with the macroscopic quantities (the diffusion and adsorption coefficients). The ''Einstein relation'' is derived that connects temporal evolution with the effective transport properties.

The model is described in Sec. II. We then demonstrate two applications, which show the relevance of hierarchical networks to modeling transport in porous media. In Sec. III the model is used as a mercury intrusion porosimetry (MIP) simulator. The MIP is widely used for measuring pore size distribution. As the results depend strongly on the connectivity of the pore space, their interpretation is not straightforward. Very sophisticated simulators have been developed for single level porous media for deconvoluting the real pore size distribution from the MIP measures [20,5]. To our knowledge, no such work has been performed in the framework of a multiscale model, apart from recent rate-controlled MIP simulations on correlated percolation networks, which showed the existence of correlated heterogeneities in sedimentary rocks [12]. We here focus on traditional pressure-controlled MIP. The image of the pore structure is qualitatively different for single scale and multiscale pore organization. A qualitative comparison of the simulation results with MIP experiments on cement pastes is given, which permits a correct interpretation of experimental data. In Sec. IV we compare the transport properties of single level and multiscale models. We focus on the role played by fractures (macropores), which have an important influence on the transport dynamics [21,22]. We show that their role is different in single level and multiscale structures. Moreover, it is seen that the reversible adsorption process, although it slows down the dynamics of the diffusion, undermines the effect of retention in fractures. We also give the scaling of a correlation length of a fractured sample as a function of the conductivity of macropores.

II. DESCRIPTION OF THE MODEL

Imagine a regular cubic network of L^3 sites. A two-dimensional section of such a network is represented in Fig. 1. Let a be the distance between two nearest neighbor sites (grid size). The nearest neighbor sites are connected by a cylinder-shaped pore of diameter d, which is randomly assigned from a distribution $f(d)$:

$$f(d)=(1-p)\,\delta(d)+ph(d), \quad 0\leqslant p\leqslant 1, \tag{1}$$

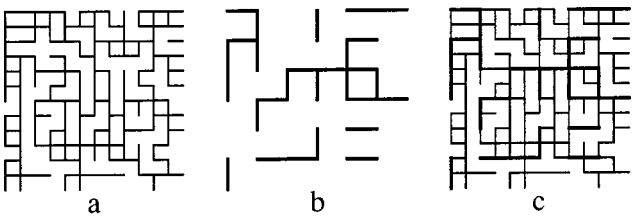

FIG. 2. Construction of the hierarchical pore network HPN with $H=2$ levels of hierarchy with the scaling factor $b=2$, $p_1=p_2=0.4$. (a) Single level network with the grid size a_1, (b) single level network with the grid size $a_2=2a_1$, and (c) the hierarchical network after the superposition of (a) and (b).

where $h(d)$ is a strictly positive distribution and $\delta(d)$ is the Dirac distribution. Consequently, a fraction $(1-p)$ of pores has a null diameter (they are absent), so that a fraction $(1-p)$ of pairs of nearest neighbor sites is not connected. The diameter of a pore connecting sites i,j is denoted d_{ij}; its section is denoted $S_{ij}=\pi(d_{ij})^2/4$.

Let the network described above represent the first level of a hierarchical pore structure. It is fully determined by the parameters L,a_1,p_1 and by the distribution $h_1(d)$. A hierarchical network with two levels is created by the superposition of this network on a similar network with the grid size a_2, where a_2 is a multiple of $a_1(a_2=ba_1)$, and with a pore size distribution $f_2(d)=(1-p_2)\,\delta(d)+p_2h_2(d)$. This process is illustrated in Fig. 2. By definition, pores on the first level that were covered during the superposition by the pores of the second level disappear. The procedure described above is iterated to obtain a network with H levels.

The basic length scale of the hierarchical network is the grid size of the network on the first level. This is also the length scale on which transport processes are defined. We thus decompose each pore on the level 2 into b *segments* of length a_1. Now two nearest neighbor sites in the network are connected by a segment.

To each segment connecting nearest neighbor sites i,j there corresponds a volume $(a_1)^3/3$ of the network. This enables us to define the *porosity* ϕ_{ij} of the segment (ij) as

$$\phi_{ij}=\frac{3S_{ij}a_1}{(a_1)^3}.$$

The porosity at site i is defined as the average value of ϕ_{ij} over the incoming segments at this site,

$$\phi_i=\frac{\sum_{\{j\}} S_{ij}a_1}{2(a_1)^3}.$$

We sum over the six nearest neighbor sites. The total volume of pores in the sample comes from two contributions: from accessible pores (the pores forming the percolation cluster [6]) and from isolated pores. As only accessible pores influence transport properties of the network, isolated pores are not considered for the definition of the total porosity Φ_0. It is evaluated as $\Phi_0=\Sigma_\Omega\phi_i(a_1)^3/V_0$, where Ω is the set of accessible sites and V_0 is the total volume of the sample.

III. MIP SIMULATIONS FOR ONE-LEVEL AND HIERARCHICAL STRUCTURES

MIP is based on the fact that the pressure we have to apply to squeeze a nonwetting fluid in a pore is inversely proportional to the diameter of this pore. For a cylindrical pore of diameter d the pressure is given by the relation [5]

$$P = -4\gamma \cos\Theta / d, \tag{2}$$

where γ is the surface energy of the liquid and Θ is the contact angle. The pore size distribution is obtained from the invaded volume measured as a function of P.

The algorithm of the intrusion, similar to the one used in invasion percolation [23,24], reflects the experimental procedure. The sample is immersed in mercury, so that the liquid can enter from all the faces. To each pressure P corresponds from Eq. (2) a diameter d, so that only the pores with $d' \geqslant d$ can be invaded. If a pore is invaded under a pressure P, its neighbors with diameter $d' \geqslant d$ are also invaded. Large networks, up to 140^3 sites, were used to minimize the finite size effects. To interpret the results, we use the function Ψ, defined by

$$\Psi(d) = \frac{1}{V_0 \Phi_0} \frac{dV(d)}{d \ln d},$$

where $V(d)$ is the cumulative volume of accessible pores having diameter $d' > d$. Then $\epsilon\Psi(d)$ gives the fraction of porosity due to the pores with diameter in the interval $[d;(1+\epsilon)d]$. The function $\Psi(d)$ reflects the real pore size distribution in the sample. Similarly, we define an ''experimental'' function $\Psi_i(d)$ as a derivative of the volume $V_i(d)$ invaded under the pressure $P(d)$. The interpretation of $\Psi_i(d)$ is not straightforward, because a fraction of pores of diameter $d' > d$ is shaded by pores of diameter $d'' < d$, so that $V_i(d) \leqslant V(d)$.

The aim of this section is twofold. First, we compare the MIP results in single level and multiscale networks. Second, we study the influence of the connectivity on the MIP results in single level and multiscale networks to find the relation between $\Psi_i(d)$ and $\Psi(d)$ that would allow a correct interpretation of the experimental data.

As we noted above, only two or three families of pores are sufficient for a correct description of a porous sample on the laboratory scale. That is why we consider a bivariate distribution of pore diameters, distributed once over a single level network and once over a hierarchical network. In the first case, the distribution is given by $f(d) = (1-p)g(d) + pg'(d)$ with $p = 0.11$; in the second case it reads $f_1(d) = g(d)$, $f_2(d) = g'(d)$ on the network with $b = 3$. The value of p is chosen in such a way that $\Psi(d)$ is the same in both cases. As the length scale is not specified, the choice of diameters is arbitrary. For simplicity, $g(d)$ and $g'(d)$ are taken to be Gaussian distributions truncated for $d \leqslant 0$, centered respectively around $m = 1$ and $m = 3$. The results obtained for networks of size 60^3 sites are presented in Fig. 3. In spite of the fact that a bivariate distribution is simulated, only one peak is present in the nonhierarchical case: macropores do not form a sample-spanning cluster, and they can be accessed only through the microporosity. This situation can be directly related to the experimental results on sandstones, where a bivariate distribution of pores is observed [18] (pores are separated by narrow necks), and only one peak is present in the MIP data [25]. In the case of intrusion in a hierarchical network two peaks are visible, because both pore families independently form a percolating cluster. The same effect is observed in the example of hardened cement paste (Fig. 7 below) where three pore families are present (capillary, micro-, and nanoporosity [19]). The network of capillary pores forms a percolating cluster even if the volumes occupied by capillary pores and micropores are comparable, which is a sign of a hierarchical structure.

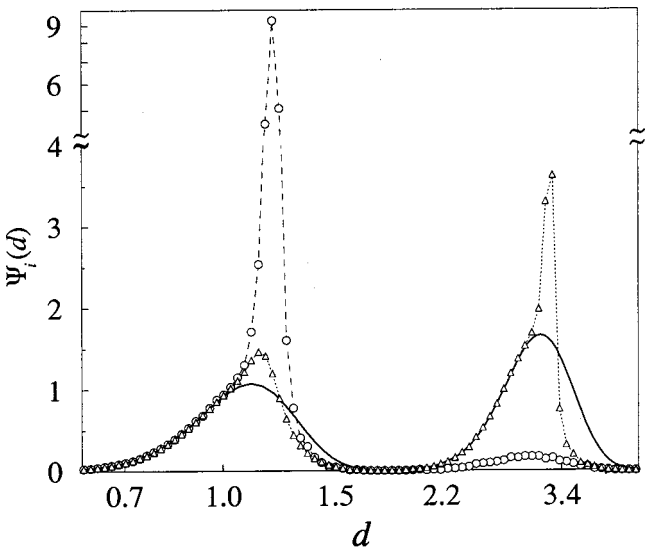

FIG. 3. Comparison of the results of simulations of mercury intrusion porosimetry for the case of pore distribution on nonhierarchical (○) and hierarchical (△, two levels, $b = 3$) networks. $\Psi(d)$ is plotted as a solid line. The diameters of the two classes of pore are given by Gaussian distributions with $m_1 = 1.0$, $\sigma_1 = 0.2$ and $m_2 = 3.0$, $\sigma_2 = 0.4$, respectively. Length scale in arbitrary units.

We can now focus on the influence of connectivity on MIP results. We first examine the case of a simple network where the pore diameters follow the distribution (1), and $h(d)$ again is a Gaussian distribution with mean m and variance σ, truncated for $d \leqslant 0$. The main part of the porosity is due to pores of diameter $d_M = \sqrt{\langle d^2 \rangle}$. If $m \gg \sigma^2$, $d_M = \sqrt{m^2 + \sigma^2}$. The distribution $\Psi_i(d)$ obtained for several values of p (Fig. 4) shows that there exists a critical diameter $d_c(p)$ that depends on p. For pressures corresponding to $d > d_c(p)$, the invaded volume of pore space is very small, even when the porosity created by pores with diameters in this range is not negligible. In fact, for $d > d_c$, invaded pores do not form a sample-spanning cluster. The observed invaded volume is thus only a finite size effect, as it corresponds to pores directly connected to the faces of the network. With increasing network size the surface-to-volume fraction goes to zero, so the fraction of invaded porosity vanishes. The value of d_c is related to the percolation threshold p_c [6] of the network through [25]

$$\int_{d_c}^{\infty} g(x)dx = \frac{p_c}{p}. \tag{3}$$

For the cubic bond percolation network $p_c \approx 0.249$ [26]. If $d < d_c$, a sample-spanning cluster of invaded pores is

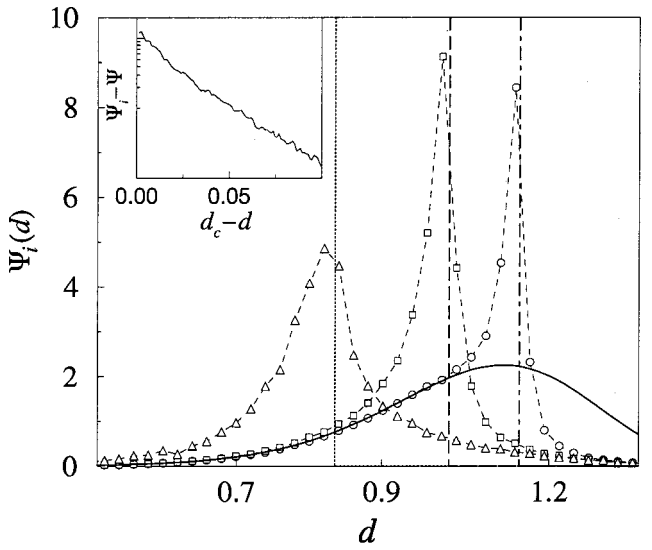

FIG. 4. Results of the simulations of mercury porosimetry intrusion on a network with a Gaussian distribution of pore diameters ($m=1$, $\sigma=0.2$). Results for $p=1$ (○), $p=0.5$ (□), and $p=0.3$ (△). Prediction (4) plotted for the three p values with dot-dashed, long-dashed, and dotted bold lines, respectively. $\Psi(d)$ plotted with solid bold line. Inset: Exponential convergence of $\Phi_i(d)$ toward $\Phi(d)$ for $d<d_c$. $p=1$ case, linear-log plot. Network of size 40^3 sites was used. Length scale in arbitrary units.

formed, so there is a high probability that the empty pores are directly connected to the invaded ones. Our numerical results indicate that (out of a very narrow critical region around d_c) $\Phi_i(d)$ converges exponentially toward $\Phi(d)$ (inset of Fig. 4). This convergence is related to the statistics of the finite clusters of pores having diameter $d' \geqslant d$. Hence we obtain $\Psi_i(d)$ approximately in the form

$$\Psi_i(d)=\begin{cases} d^3 g(d)/\langle d^2\rangle & \text{for} \quad d<d_c \\ \left(\int_{d_c}^{\infty} x^3 g(x)dx/\langle d^2\rangle\right)\delta(d-d_c) & \text{for} \quad d\geqslant d. \end{cases} \tag{4}$$

Equation (4) very well approximates the simulation results for p far enough from p_c. As shown by previous analysis, for $d>d_c$ we lose *all* the information about the distribution. It is also important to note that the value of d_c corresponding approximately to the peak of $\Psi_i(d)$, is not equal to d_M [the peak of $\Psi(d)$]. If the network of pores approaches the percolation threshold, d_c is *significantly lower* than d_M.

The results of intrusion in a hierarchical network are presented in Figs. 5 and 6. A network with three levels is used. First, three levels are of sufficient generality for observation of the effects of the hierarchical structure on MIP results. Secondly, use of three levels allows a direct comparison of the simulation results with the experimental data for hardened cement pastes, where three families of pores are encountered [19]. Simulations were done on a network of 128^3 sites with the scaling factor $b=2$. The pore size distribution on each level follows Eq. (1). Let $g(d)$ again be a truncated Gaussian distribution, with, respectively $m_1=1$, $\sigma_1=0.2$, $m_2=2$, $\sigma_2=0.4$, and $m_3=4$, $\sigma_3=0.2$. The parameters were chosen to obtain three distinct families of pores, which will be called nanoporosity, microporosity, and macroporosity.

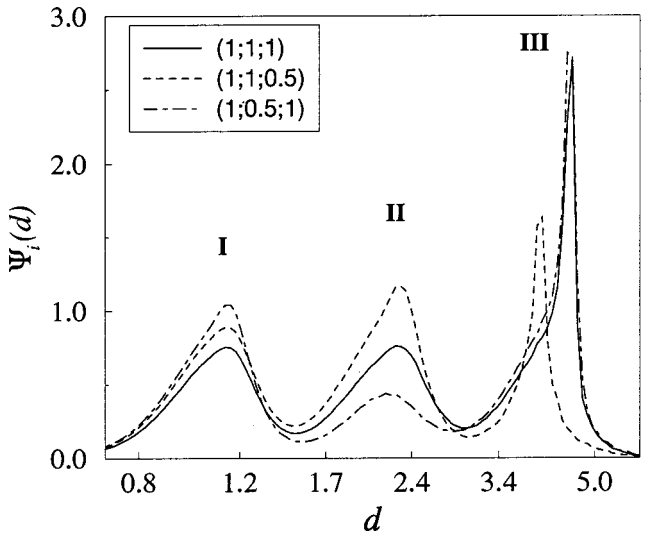

FIG. 5. Variation of $\Psi_i(d)$ with the connectivity of the network. Three-level network with $b=2$. Pore diameters of the three pore classes are given by a truncated Gaussian distribution, with, respectively, $m_1=1.0$, $\sigma_1=0.2$, $m_2=2.0$, $\sigma_2=0.4$, and $m_3=4.0$, $\sigma_3=0.8$. Length scale in arbitrary units.

The peaks corresponding to these pore families are denoted, respectively, I, II, and III. The connectivity is fixed by the triplet (p_1,p_2,p_3).

The comportment of the macroporosity peak can be directly deduced from the preceding results obtained for a nonhierarchical network. If the connectivity of the network of macropores decreases, the position of this peak shifts toward smaller diameters (Fig. 5). The behavior of the other peaks depends on the global connectivity of the network. In the case of a well connected network, the position of the peaks I and II does not depend on the connectivity of macropores. The maximum of each of these peaks always indicates the characteristic diameter of the corresponding family of pores [cases (1;1;1) and (1;1;0.5) in Fig. 5]. Peak II shifts only once the macropore network no longer forms a percolating cluster. Its position is then determined by the

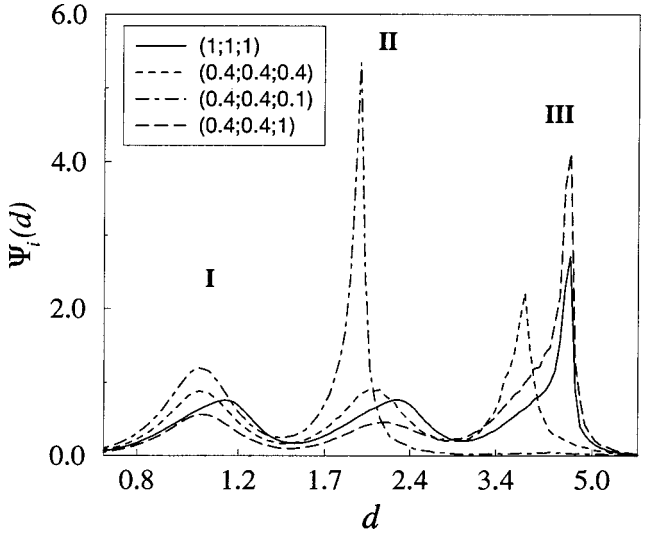

FIG. 6. Variation of $\Psi_i(d)$ with the connectivity of the network. For the details, see Fig. 5.

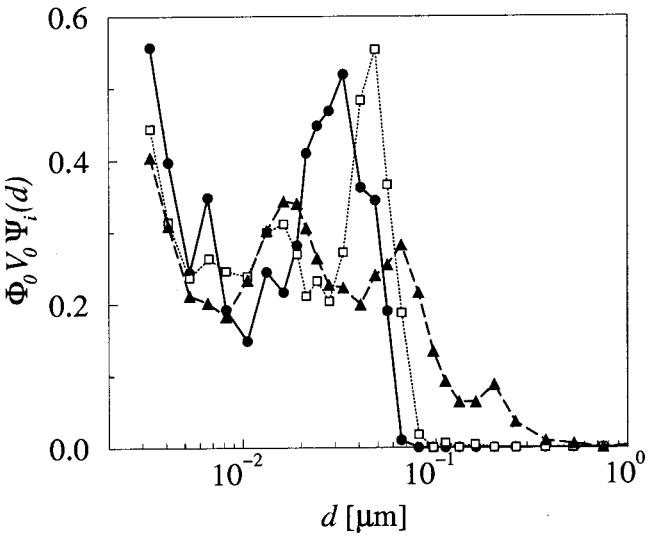

FIG. 7. Results of MIP experiments in hardened cement paste for different w/c ratios: $w/c=0.5$ (▲), $w/c=0.4$ (□), $w/c=0.3$ (●).

relation (3), where the value of p_c corresponds to the percolation threshold of the network formed by both micropores and macropores. In the case where only the connectivity of the micropores decreases [case (1;0.5;1)], the peak II does not shift toward smaller diameters, because the network of micropores is always well connected via the network of macropores. This is true also for the nanopores.

In the case of a weakly connected network, the influence of the different families of pores is no longer uncorrelated (Fig. 6). If the connectivity decreases homogeneously $[(1;1;1)\rightarrow(0.4;0.4;0.4)]$, the positions of all the peaks change. The shift of peak III is the most important, but peaks I and II are also shifted toward smaller diameters, because the weakly connected network of macropores cannot compensate the weak connectivity of micropores and nanopores. Moreover, in this case the connectivity of macropores influences the position of the microporosity peak. If the connectivity of the network of macropores increases, peak II is shifted toward the higher diameters [case (0.4;0.4;1)]; if it decreases, this peak moves toward the lower diameters [case (0.4;0.4;0.1)].

The results presented were obtained for networks with $b=2$. The situation is different if $b\gg 2$. Because of computation limits this case is not accessible for the simulations; nevertheless, the behavior can be deduced from the preceding results. In this case pores on level i occupy large regions that are not intersected by the pores on level $j>i$. Hence the percolationlike effects affect all the pore classes, and the position of a peak in MIP results depends only on the connectivity of the corresponding pore class.

In conclusion, for well connected networks only the rightmost peak in the MIP results is strongly affected by percolationlike effects. The positions of the other peaks indicate correct diameters of the corresponding pore classes. Moreover, Eq. (3) shows that the porosity indicated by the rightmost peak may be partially due to the unconnected pores having diameter $d>d_c$. The effects described are observable in experimental results. In Fig. 7 we show the results obtained on CEM-I pastes for different water-to-cement ratios (w/c). Variation of w/c mainly affects the position of the rightmost peak; the position of the central peak is practically unchanged. From analysis of the porosity indicated by the rightmost peak, it is readily seen that its displacement is due not only to a decreased average diameter of pores, as could be concluded, but also to a decreased connectivity [27].

IV. TRANSPORT IN NONHIERARCHICAL VERSUS HIERARCHICAL POROUS MEDIA

A. Diffusion-adsorption process

The diffusion process in the network is defined by the microscopic motion of particles. A particle can be found at site i of the network with a probability P_i. It can be either diffusing (probability P_i^f) or adsorbed (probability P_i^a). We have $P_i=P_i^f+P_i^a$. A diffusing particle at site i can either jump to the nearest neighbor site j with the probability W_{ij} or be adsorbed with the probability γ_i^a. An adsorbed particle is released with probability γ_i^r. The diffusion process is described by means of a pair of balance equations (master equations):

$$\frac{\partial P_i^f}{\partial t}=\sum_{\{j\}}\left(W_{ji}P_j^f-W_{ij}P_i^f\right)+P_i^a\gamma_i^r-P_i^f\gamma_i^a, \tag{5}$$

$$\frac{\partial P_i^a}{\partial t}=\gamma_i^a P_i^f-\gamma_i^r P_i^a.$$

In three dimensions the macroscopic diffusion coefficient D is defined through the relation [28]

$$\overline{\langle \mathbf{R}^2(t)\rangle}=6Dt, \tag{6}$$

where $\mathbf{R}(t)$ is the distance of the particle from origin at time t, and $\langle\cdots\rangle$ means the average computed over all possible random walks on a given network. The overbar, represents the average calculated over all possible realizations of the network.

The transition rates W_{ij}, γ_i^r, and γ_i^a are found by comparison of Eq. (5) with the diffusion equation in porous media [29],

$$\phi(\mathbf{x})(1+K^{ad})\partial_t c^f(\mathbf{x},t)=\nabla\cdot[\phi(\mathbf{x})D(\mathbf{x})\nabla c^f(\mathbf{x},t)]. \tag{7}$$

Here D_e is the effective diffusion coefficient, c^f is the concentration of diffusing particles in the pore, and K^{ad} is the adsorption/desorption coefficient, expressed in the form

$$K^{ad}(\mathbf{x})=\frac{\alpha(\mathbf{x})}{\phi(\mathbf{x})}k_{eq}, \tag{8}$$

where $\alpha(\mathbf{x})$ is the specific surface of the pore and k_{eq} is the ratio of the concentrations of adsorbed and diffusing particles at equilibrium. The probability P_i^f is expressed by means of the concentration, $c_i^f=P_i^f/[\phi_i(a_1)^d]$, and the adsorption/desorption coefficient K^{ad} is introduced, $K_i^{ad}=\gamma_i^a/\gamma_i^r$. If the variations of $\partial P_i^t/\partial t$ are slow enough $(\partial^2 P_{ij}^t/\partial t^2\simeq 0)$, Eq. (5) simplifies to

$$\phi_i(1+K_i^{ad})\frac{\partial c_i^f}{\partial t}=\sum_{\{j\}}\left(\phi_j W_{ji}c_j^f-\phi_i W_{ij}c_i^f\right)$$

$$=\sum_{\{j}\phi_i W_{ij}(c_j^f-c_i^f). \qquad (9)$$

The equality $\phi_j W_{ji}=\phi_i W_{ij}$ results from the fact that the concentration has to be constant in the stationary state. Comparison of Eqs. (9) and (7) yields

$$(a_1)^2\phi_i W_{ij}=D(\mathbf{x})\phi(\mathbf{x}),\quad K_i^{ad}=K^{ad}(\mathbf{x}). \qquad (10)$$

The diffusion coefficient in the network can be measured directly using Eq. (6), or indirectly, by calculating the conductivity Σ of the equivalent electrical network and using an ''Einstein relation'' for the evaluation of D [4,30,31]. The equivalent electrical network is built by replacing the pores with resistances having the conductivity $\sigma_{ij}=a_1\phi_i W_{ij}$. Using a simple generalization of Derrida *et al.*, demonstration of the equivalence between the diffusion and conductivity problems [32], it can be shown that D and Σ are then related through $\Sigma=\langle\phi_i(1+K_i^{ad})\rangle D$, where $\langle\cdots\rangle$ is the average calculated over the network. In the same manner, the relation between D and the effective diffusion coefficient D_e is found. This last coefficient, usually experimentally accessible, measures the flux $\mathbf{Q}$ through the sample in steady state. It is defined through Fick's law $\mathbf{Q}=-D_e\nabla c$. The relation between D and D_e reads

$$D_e=\langle\phi(1+K^{ad})\rangle D. \qquad (11)$$

The relations between D, D_e, and Σ are of both practical and theoretical importance. First, it is relatively easy to evaluate the the electrical conductivity of a network, since special algorithms for this purpose have been developed [33,34]. Second, it is simpler to discuss the transport properties of a pore network by means of the ''conductivity'' of pores σ_{ij} than by means of the diffusive flux through a pore, which, as seen from Eq. (10), is a function of two independent parameters $D(\mathbf{x})$ and $\phi(\mathbf{x})$.

B. D and D_e in hierarchical and nonhierarchical networks

We can compare the diffusion coefficients D and D_e in hierarchical and nonhierarchical networks with two families of pores, (micropores and macropores). In such a network the porosity can be varied in several ways. We chose to fix the microporosity, and to vary the porosity by adding macropores. This corresponds to measuring the diffusion coefficient in several samples of a medium that are fractured to different extents, or in samples of hardened cement pastes with different water-to-cement ratios w/c. The pore diameters in the network are then given by the distribution

$$f(d)=(1-p')\delta(d-d_1)+p'\delta(d-d_2),\quad p'\in[0;1/9], \qquad (12)$$

for the nonhierarchical network, and by

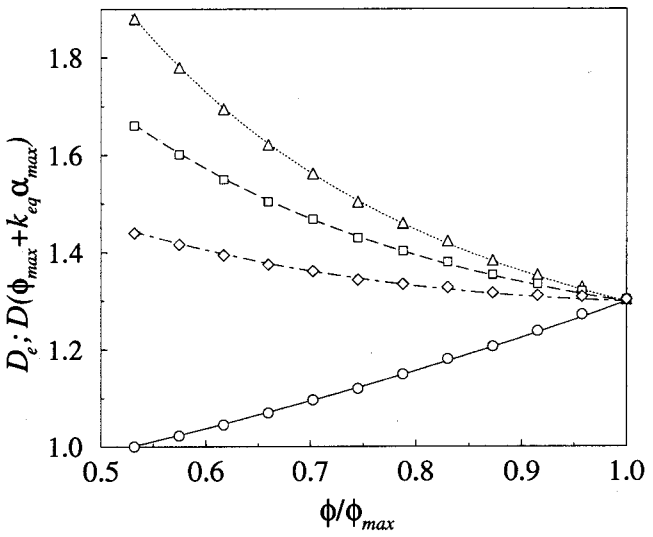

FIG. 8. Diffusion coefficient of a nonhierarchical network. D_e (○); D with $k_{eq}=0$ (△), $k_{eq}=0.125$ (□), and $k_{eq}=0.5$ (◇). Length scale in arbitrary units. Lines represent the EMA results.

$$f_1(d)=\delta(d-d_1),$$

$$f_2(d)=(1-p)\delta(d)+p\delta(d-d_2),$$

$$p\in[0;1], \qquad (13)$$

for the hierarchical network. The porosity is tuned by the parameters p and p'. If $p'=p/9$, the pore size distributions are identical in the two networks. The porosity ϕ then varies in the interval $[\phi_{min};\phi_{max}]$, where $\phi_{min}=3\pi(d_1/2a_1)^2$ and $\phi_{max}=3\pi(8d_1^2+d_2^2)/36a_1^2$ (a_1 is the grid size of the network). The specific surface varies in the interval $[\alpha_{min};\alpha_{max}]$, where $\alpha_{min}=3\pi d_1/a_1^2$ and $\alpha_{max}=\pi(8d_1+d_2)/3a_1^2$.

Since the length scale is not specified, this choice of the diameters d_1, d_2 is arbitrary. We choose $d_1=1$, $d_2=3$. The value $b=3$ is used, so the aspect ratio of pores is constant in the hierarchical network. The conductivity σ of a pore should be proportional to its section, $\sigma=d^2$. This corresponds to the assumption that the diffusion coefficient in a pore does not depend on its diameter. Networks of sizes up to 60^3 sites were used for the calculations. In all the cases we checked that the size of the network was larger than the correlation length, so finite size effects are not important.

The simulation results for the nonhierarchical network, together with the effective medium approximation (EMA) results [35], are shown in Fig. 8. The value of the effective diffusion coefficient D_e increases with the porosity. In contrast, the value of the diffusion coefficient D decreases: the presence of macropores slows down the diffusion, because they act as reservoirs of particles. It takes a relatively long time for the concentration to equilibrate between the macropore and its surroundings. It is noteworthy that this effect is important only in the regime of weak adsorption. As $K^{ad}\sim k_{eq}/d$, the adsorption is stronger in pores with smaller diameter. If k_{eq} grows, the effect of ''trapping'' in macropores is then partially compensated by the adsorption in micropores.

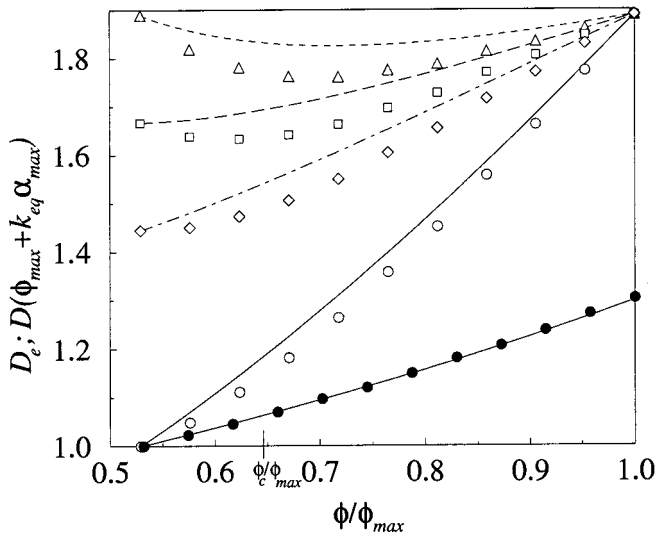

FIG. 9. Diffusion coefficient of a hierarchical network. D_e (○); $D(\phi_{max}+k_{eq}\alpha_{max})$ with $k_{eq}=0$ (△), $k_{eq}=0.125$ (□), and $k_{eq}=0.5$ (◇). D_e of the nonhierarchical network plotted for comparison (●). p_c indicates the percolation threshold of the network of macropores. Length scale in arbitrary units. Lines represent the EMA results.

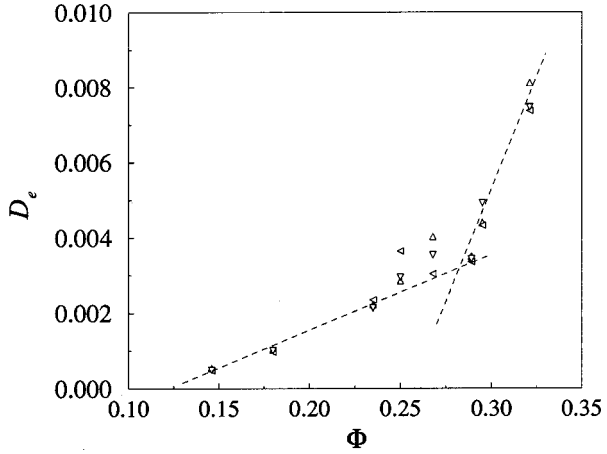

FIG. 10. Effective diffusion coefficient measured for CEM-I hardened cement pastes.

Because of the correlations in the pore size distribution, we cannot directly apply the EMA on the hierarchical network. Nevertheless, it is possible to use the ''decimation'' method described in [15], where a cell of size ba_1 is replaced by an effective bond with a rescaled conductivity. If we denote by σ_m and σ_M, respectively, the conductivity of micropores and macropores, the conductivity of the effective bond is $\sigma'_M=[\sigma_M+(b^2-1)\sigma_m]/b^2$ with a probability p, and $\sigma'_m=\sigma_m$ with a probability $(1-p)$. Because the correlations disappear in the resulting network, the EMA can be applied. The EMA result are lower than in the preceding case, but the qualitative features are reproduced well (Fig. 9). A change in the slope of D_e is seen around $\phi=\phi_c$, where the percolating cluster of macropores is initially formed. As the values of σ'_m and σ'_M are of the same order, this effect is not pronounced. It becomes more important if the ratio σ'_m/σ'_M increases. In Fig. 10 we plot the experimental results for hardened cement pastes obtained with different water-to-cement ratios. Here σ'_M corresponds to the diffusion in a fully hydrated paste without capillary pores and σ'_m to the diffusion coefficient in capillary pores (in water). As $\sigma'_M/\sigma'_m\sim 100$, the change of slope of D_e is pronounced. The value of the percolation threshold of capillary porosity $\phi_c\approx 0.3$ is compatible with the MIP results (Fig. 7). For the process with weak adsorption, the value of D decreases with the porosity for $\phi<\phi_c$ (Fig. 9). If the network of macropores becomes connected, the diffusion is accelerated if the porosity increases. As in the case of the nonhierarchical network, the effect of trapping in macropores is less pronounced in the presence of adsorption.

C. Correlation length

An important issue in transport in porous media is the correlation length ξ in the sample. Only if the size of the sample $L>\xi$ are the measured transport coefficients scale independent so that their values can be extrapolated. In a network with a bivariate distribution of pore sizes, there are two points where ξ becomes important. The first point is the percolation threshold of the network. The behavior of ξ in its vicinity is well understood from percolation theory [6]. The second point of interest is the percolation threshold of the macroporosity. Here the network of macropores becomes fractal, and its correlation length diverges. Nevertheless, the presence of micropores assures the finiteness of ξ of the complete network, and the evolution of ξ varies as a function of the conductivity of macropores. We treat the single level network case first; then we show that the same approach can be generalized to the hierarchical case.

Let the pore size distribution be given by Eq. (12). We denote the conductivity of micropores and macropores as σ_m and σ_M, respectively. Let the network of macropores be at the percolation threshold, $p=p_c$. We introduce a parameter ρ as the ratio of σ_m and σ_M, $\rho=\sigma_m/\sigma_M$. If $\rho=1$, $\sigma_m=\sigma_M$, and thus $\xi=1$. If $\rho\to\infty$, a percolation network is obtained, where macropores behave as (super)conductors, micropores as insulators. As $p=p_c$, the correlation length diverges, $\xi\to\infty$. This behavior is compatible with an algebraic dependence of ξ on ρ,

$$\xi=\rho^{-\alpha}. \tag{14}$$

The conductivity evolves with the correlation length according to the relation [6]

$$\frac{\Sigma}{\sigma_M}=L^{-\mu/\nu}F\left[\left(\frac{L}{\xi}\right)^{\mu/\nu}\right]=L^{-\mu/\nu}F(\rho^{\alpha\mu/\nu}L^{\mu/\nu}), \tag{15}$$

where the scaling function $F(x)$ satisfies $F(0)=1$, $\lim_{z\to\infty}F(z)\propto z$, and μ,ν are the critical exponents of the conductivity and correlation length. The value of exponent α is obtained from the evolution of Σ for $L\to\infty$, where $\Sigma/\sigma_M\sim\rho^{\mu/(\mu+s)}$ [36], s being the ''superconductivity'' exponent [6]; $s=\mu$ in two dimensions but $s\neq\mu$ in three di-

mensions. Then from Eq. (15) we have $\alpha=\nu/(\mu+s)$. In three dimensions $\nu=0.88$, $\mu=2.0$, and $s=0.73$, so $\alpha=0.32$.

As mentioned above, traditional methods cannot be directly applied in the hierarchical network case because of the presence of correlations. Nevertheless, the hierarchical network with a scaling factor b has the same behavior as an ordinary percolation network with the rescaled conductivities Σ'_M and σ'_m. The correlation length at the percolation threshold of macropores then behaves as $\xi\sim(\Sigma'_m/\Sigma'_M)^{-\alpha}$. It is worth noting that the correlation length is not only a geometrical property of a network, but also depends on the dynamical process considered. For example, it will be different for a diffusion process, where the conductivity of a pore is typically proportional to its section, $\sigma_{ij}\sim d_{ij}^2$, and for permeability, where the conductivity is given by the Poisseulle law, $\sigma_{ij}\sim d_{ij}^4$ [25].

V. CONCLUSION

In this article we compared the transport properties of porous media with hierarchical and with nonhierarchical organization of pores. We developed a description of the diffusion or adsorption processes in a pore network model. This allows the study not only of the effective transport coefficients, but also of the evolution of the diffusion processes in time. We found a relationship between the microscopic transport process and the macroscopic diffusion equation, which links the transition rates to the macroscopic coefficients. The probabilities of adsorption and desorption γ^a and γ^r determine the time scale of the adsorption-desorption processes. It is worth remarking that in the diffusion equation (7) they are present only in the form of their ratio, $K^{ad}=\gamma^a/\gamma^r$. Thus the time scale of the adsorption-desorption processes is lost, and Eq. (7) is valid only under the hypothesis that equilibrium between the concentration of adsorbed and free particles is reached instantaneously. The influence of the adsorption dynamics on the temporal evolution of the transport process should also be investigated.

MIP gives an incomplete description of the pore size distribution, because samples with different pore size distributions can lead to similar MIP results. We showed that the MIP data cannot be interpreted with simple MIP simulators, because they depend on the connectivity of pores on different scales. In spite of these shortcomings, MIP gives valuable indications about the pore size distribution in sample. It allows an experimental distinction between the hierarchical and nonhierarchical organization of pores, and it furnishes information about the connectivity properties of the pore space, which is important information for transport studies. Comparison of our simulation results with experimental data shows the necessity of the introduction of correlations in the pore size distribution for correct modeling of certain porous media.

ACKNOWLEDGMENTS

We thank Jérôme Chave and Pierre Evesque for fruitful discussions and for a careful reading of the manuscript. We thank also Chrisophe Gallé and Michel Pin for allowing us to use some of their experimental results.

[1] B.I. Halperin, S. Feng, and P.N. Sen, Phys. Rev. Lett. **54**, 2391 (1985).
[2] S.C. van der Marck, Phys. Rev. Lett. **77**, 1785 (1996).
[3] I. Fatt, Trans. AIME **207**, 144 (1956).
[4] J. Koplik, S. Redner, and D. Wilkinson, Phys. Rev. A **37**, 2619 (1988).
[5] M. Sahimi, Rev. Mod. Phys. **65**, 1393 (1993).
[6] D. Stauffer and A. Aharony, *Introduction to Percolation Theory* (Taylor & Francis, Washington, D.C., 1992).
[7] S. Bryant and M. Blunt, Phys. Rev. A **46**, 2004 (1992).
[8] C. Clauser, EOS Trans. Am. Geophys. Union **73**, 223 (1992).
[9] B.D. Hughes and M. Sahimi, Phys. Rev. Lett. **70**, 2581 (1993).
[10] B.D. Hughes and M. Sahimi, Phys. Rev. E **48**, 2776 (1993).
[11] M. Sahimi and S. Mukhopadhyay, Phys. Rev. E **54**, 3870 (1996).
[12] M.A. Knackstedt, A.P. Sheppard, and W.V. Pinczewski, Phys. Rev. E **58**, R6923 (1998).
[13] A.V. Neĭmark, Zh. Éksp. Teor. Fiz. **96**, 1386 (1989) [Sov. Phys. JETP **69**, 786 (1989)].
[14] K. Xu, J.-F. Daian, and D. Quenard, Transp. Porous Media **26**, 52 (1997).
[15] P. Gavrilenko and Y. Guéguen, Water Resour. Res. **34**, 177 (1998).
[16] E. Perrier, C. Mullon, and M. Rieu, Water Resour. Res. **31**, 2927 (1995).
[17] Henri Van Damme, C. R. Acad. Sci., Ser. IIa: Sci. Terre Planetes **320**, 665 (1995).
[18] F.A.L. Dullien and G.K. Dhawan, J. Colloid Interface Sci. **52**, 129 (1975).
[19] H. F. W. Taylor, *Cement Chemistry* (Academic Press, New York, 1990).
[20] C.D. Tsakiroglou and A.C. Paytakes, J. Colloid Interface Sci. **137**, 315 (1990).
[21] M.R. Homp and J. David Logan, Transp. Porous Media **29**, 341 (1997).
[22] I. Neretnieks, J. Geophys. Res. B **85**, 4379 (1980).
[23] D. Wilkinson and J.F. Willemsem, J. Phys. A **16**, 3365 (1983).
[24] M.M. Dias and D. Wilkinson, J. Phys. A **19**, 3131 (1986).
[25] A.J. Katz and A.H. Thompson, Phys. Rev. B **34**, 8179 (1986).
[26] D.G. Gingold and C.J. Lobb, Phys. Rev. B **42**, 8220 (1990).
[27] R. Vočka, C. Gallé, M. A. Dubois, and P. Lovera (unpublished).
[28] J.W. Haus and K.W. Kehr, Phys. Rep. **150**, 263 (1987).
[29] O. A. Plumb and S. Whitaker, in *Dynamics of Fluids in Hierarchical Porous Media*, edited by J. H. Cushman (Academic Press, New York, 1990), pp. 97–148.
[30] D.L. Johnson and P.N. Sen, Phys. Rev. B **37**, 3502 (1988).
[31] P. Wong, J. Koplik, and J.P. Tomanic, Phys. Rev. B **30**, 6606 (1984).

[32] B. Derrida, J. P. Bouchaud, and A. Georges, in *Disorder and Mixing*, edited by Etienne Guyon, Jean Pierre Nadal, and Yves Pomeau (Kluwer Academic Publishers, Dordrecht, 1988).
[33] R. Fogelholm, J. Phys. C **13**, L571 (1980).
[34] D.J. Frank and C.J. Lobb, Phys. Rev. B **37**, 302 (1988).
[35] S. Kirkpatrick, Phys. Rev. Lett. **27**, 1722 (1971).
[36] A.L. Efros and B.I. Shklovskii, Phys. Status Solidi B **76**, 475 (1976).